Journal of Experimental Botany, Vol. 58, No. 6, pp. 1451–1461, 2007
doi:10.1093/jxb/erm007 Advance Access publication 24 February, 2007
This paper is available online free of all access charges (see http://jxb.oxfordjournals.org/open_access.html for further details)

Journal of Experimental Botany
www.jxb.oxfordjournals.org

RESEARCH PAPER

Novel efficient methods for measuring mesophyll anatomical characteristics from fresh thick sections using stereology and confocal microscopy: application on acid rain-treated Norway spruce needles

Jana Albrechtová[1,2,*], Jiří Janáček[3], Zuzana Lhotáková[1,3], Barbora Radochová[3] and Lucie Kubínová[3]

[1] *Charles University in Prague, Faculty of Science, Department of Plant Physiology, Viničná 5, CZ-12844, Prague 2, Czech Republic*

[2] *Institute of Botany, Academy of Sciences of the Czech Republic, CZ-25246 Průhonice, Czech Republic*

[3] *Department of Biomathematics, Institute of Physiology, Academy of Sciences of the Czech Republic, Vídeňská 1083, CZ-14220, Prague 4, Czech Republic*

Received 22 June 2006; Revised 18 December 2006; Accepted 22 December 2006

Abstract

Recent design-based stereological methods that can be applied to thick sections cut in an arbitrary direction are presented and their implementation for measuring mesophyll anatomical characteristics is introduced. These methods use software-randomized virtual 3D probes, such as disector and fakir test probes, in stacks of optical sections acquired using confocal microscopy. They enable unbiased estimations of the mean mesophyll cell volume, mesophyll cell number in a needle, and for the first time an internal surface area of needles or other narrow leaves directly from the fresh tissue cross-sections cut using a hand microtome. Therefore, reliable results can be obtained much faster than when using a standard microtechnical preparation. The proposed methods were tested on Norway spruce needles affected for 1 year by acid rain treatment. The effect of acid rain resulted in changes of mesophyll parameters: the ratio of intercellular spaces per mesophyll cell volume increased, while needle internal surface area, total number of mesophyll cells, and number of mesophyll cells per unit volume of a needle decreased in the treated needles.

Key words: Confocal microscopy, disector method, fakir method, internal surface area, mesophyll, Norway spruce, stereology.

Introduction

Internal leaf structure, which is connected with the process of photosynthesis because it influences the interception of light and diffusion of CO_2, is known to be affected by the environment. Recent studies show that relationships between leaf anatomy parameters and photosynthesis are important in leaf acclimation to high or low irradiances (Pandey and Kushwaha, 2005) or elevated CO_2 concentrations (Eguchi *et al*., 2004).

The first quantitative descriptions of leaf anatomy (Pazourek, 1988) were based on counting planar features, especially counting stomata per unit area of the leaf (stomata density). In the first half of the 20th century, methods for quantifying internal leaf structure, such as cell volume and cell surface area per unit volume of leaf tissue, emerged (Turrell, 1936). These methods were model based, i.e. they assumed that mesophyll cells have specific shapes of simple geometric bodies. However, such model-based methods are usually biased because the shape of mesophyll cells is often irregular, thus strongly deviating from the model geometrical bodies, and so the measurements can lead to unreliable and imprecise results.

Development of stereological methods during the second half of the 20th century brought new approaches that could be applied to quantitative analysis of internal leaf structure (Weibel, 1979; Howard and Reed, 1998). The stereological point-counting method for measuring volume density or volumetric proportion of leaf tissues

* To whom correspondence should be addressed. E-mail: albrecht@natur.cuni.cz

has become widely used (Chabot and Chabot, 1977; Pazourek, 1977; Parkhurst, 1982; Albrechtová and Kubínová, 1991; Kubínová, 1991, 1993).

Corresponding stereological methods were established for surface area measurements, such as cell surface area exposed to intercellular spaces [usually expressed per unit leaf area, *A(mes)*/*A*]; however, some assumptions about the cell shape were often still made, for example, a specific shape factor for the given population of cells had to be applied (Parkhurst, 1982; Slaton and Smith, 2002; Rhizoupoulou and Psaras, 2003).

Design-based, assumption-free stereological methods, enabling unbiased evaluation of the structure of three-dimensional (3D) objects of arbitrary shapes, however, were developed and adapted to evaluate leaf tissues. The proposal to estimate the mesophyll cell surface area exposed to intercellular spaces (i.e. internal leaf surface area) using a design-based stereological method of vertical sections (Kubínová, 1991, 1993) was not used by other authors.

The situation is similar for counting mesophyll cells or measuring their mean volume. Most developed methods were again model based (Chonan, 1965; Wilson and Cooper, 1967; Sasahara, 1982), or the number of cells was determined by counting isolated cells (Maksymowych, 1959; Sasahara, 1982; Lieckfeldt, 1989), which may lead to the loss of cells during the manipulation of the cell suspension or by damage to certain cells. The design-based stereological disector method (Sterio, 1984) has not found wide application in plant anatomical studies, although its application to count mesophyll cells has been worked out (Albrechtová and Kubínová, 1991; Kubínová, 1991, 1993).

Considering that the reliable but laborious methods proposed in the 1990s have only rarely been applied, there is a clear need for less demanding, efficient, and unbiased methods for measuring physiologically important mesophyll anatomical characteristics, such as internal leaf surface area, mean mesophyll cell volume, and cell number in the leaf. The recently developed methods, based on confocal stereology, appear to be suitable for this purpose because they are efficient, unbiased, and can be applied to thick fresh tissue sections, thus minimizing time spent on tissue specimen preparation.

Confocal stereology is a contemporary approach that evaluates structures using a combination of stereological methods and confocal microscopy (Pawley, 1995), enabling perfectly registered stacks of thin serial optical sections (~350 nm thick) within thick specimens to be obtained. Digital images of such stacks represent suitable 3D image data for quantitative measurements. Howard *et al*. (1985) presented the first application of confocal microscopy to stereological measurements in their concept of an unbiased sampling brick. Confocal microscopy proved to be useful especially in the application of stereological methods based on spatial estimators that evaluate small 3D samples of the structure under study (Howard *et al*., 1985; Howard and Sandau, 1992; Kubínová and Janáček, 1998; Kubínová *et al*., 1999, 2002). A 3D sample of examined tissue can be analysed if a rectangle within a microscope's field of view is focused through. Using special software, different virtual test probes with an arbitrary predefined (e.g. random) position and orientation can be generated within the stack of sections and can be applied directly to these 3D image data. This study presents the confocal stereological methods used to evaluate the mesophyll structure of narrow leaves, such as conifer needles. The mean mesophyll cell volume and cell number in a needle are estimated using the optical disector method (Gundersen, 1986), and the internal needle surface area (defined as the surface area of mesophyll cell walls exposed to intercellular spaces) using the fakir method (Kubínová and Janáček, 1998). Unlike classical stereological methods applied to thin physical sections, the fakir method does not require randomization of the orientation of the section, hence the physical thick sections can be cut in an arbitrary direction. Therefore, the slices were cut perpendicular to the main axis of the needle, which is most suitable from the technical point of view.

Further, it was checked whether classical stereological methods can also be applied to images captured using confocal microscopy. The implementation of the point-counting method (Weibel, 1979) and Cavalieri principle (Gundersen and Jensen, 1987) for estimating the needle volume, volume density of needle tissues, and their cross-sectional areas is presented.

The aims of the present study include the following: (i) to test the usability of thick fresh needle sections cut using a hand microtome without any pre-processing for confocal microscopy and subsequent application of stereological methods applied to a series of optical sections; (ii) to estimate the stereological parameters that characterize the anatomical structure of mesophyll of Norway spruce needles; and (iii) to find out if the selected anatomical parameters are able to capture subtle changes in needle anatomy induced by acid rain treatment.

Materials and methods

Plant material and simulated acid rain treatment

Sun-exposed needles from the upper whorl of one potted 5-year-old Norway spruce (*Picea abies* L. Karst.) were used as plant material for this study. The tree was located in the botanical garden of the Department of Plant Physiology, Charles University in Prague. The first batch of five first-year needles from one branch of the experimental tree was sampled in January 1999. These needles were used as an untreated control sample. After needle sampling, the tree was treated for 1 year with a solution (pH 2.9 containing 66.0 mg dm^{-3} SO_4^{2-}, 18.6 mg dm^{-3} NO_3^-, 6.0 mg dm^{-3} NH_4^+) to

simulate the precipitation quality of acid rain (SAR) monitored in the Krkonoše Mountains at the beginning of the 1990s (Vávra, 1992). The second batch of five first-year needles from the same branch was sampled in January 2000 after 1 year of treatment.

Sample preparation and confocal microscopy

Thick transverse needle sections were cut in positions sampled according to the principle of systematic uniform random sampling (Kubínová, 1991), as shown in Fig. 1A, immediately after needle collection. Because needle length, which was measured first, was ~10 mm in both variants, the interval between sampled sections was chosen to be 2 mm, resulting in five thick sections per needle available for further analysis. The sections, ~60 μm thick, were cut using a hand microtome. A position, z, of the first section was randomly selected within the 2 mm interval (Fig. 1A). Sections were placed into distilled water between two cover glasses without any staining or other pre-processing—only autofluorescence of chlorophylls and phenolic compounds in the cell walls was exploited.

A series of 40 optical sections, 1 μm apart (Fig. 1B), was acquired using a Bio-Rad MRC600 laser scanning confocal microscope using excitation with the Kr/Ar laser at a wavelength of 488 nm and an emission range above 515 nm, and a Nikon water immersion planapochromat objective (×60, NA=1.2) to ensure that the refractive indices of the tissue and the immersion fluid matched. On average, 22 fields of view (211 μm×141 μm), selected using the systematic uniform random sampling (Fig. 1C, see also Fig. 7 in Kubínová, 1994), were captured per needle. The positions of these fields of view were set using Modig 105 potentiometric sensors (Megatron Elektronik AG & Co., Munich, Germany) attached to the microscope stage.

To measure needle volume and the volume density of mesophyll (i.e. mesophyll volume per unit volume of the needle) and other needle tissues, images of entire needle sections (Fig. 2) were collected using a ×4 Nikon dry planachromat objective (NA=0.1).

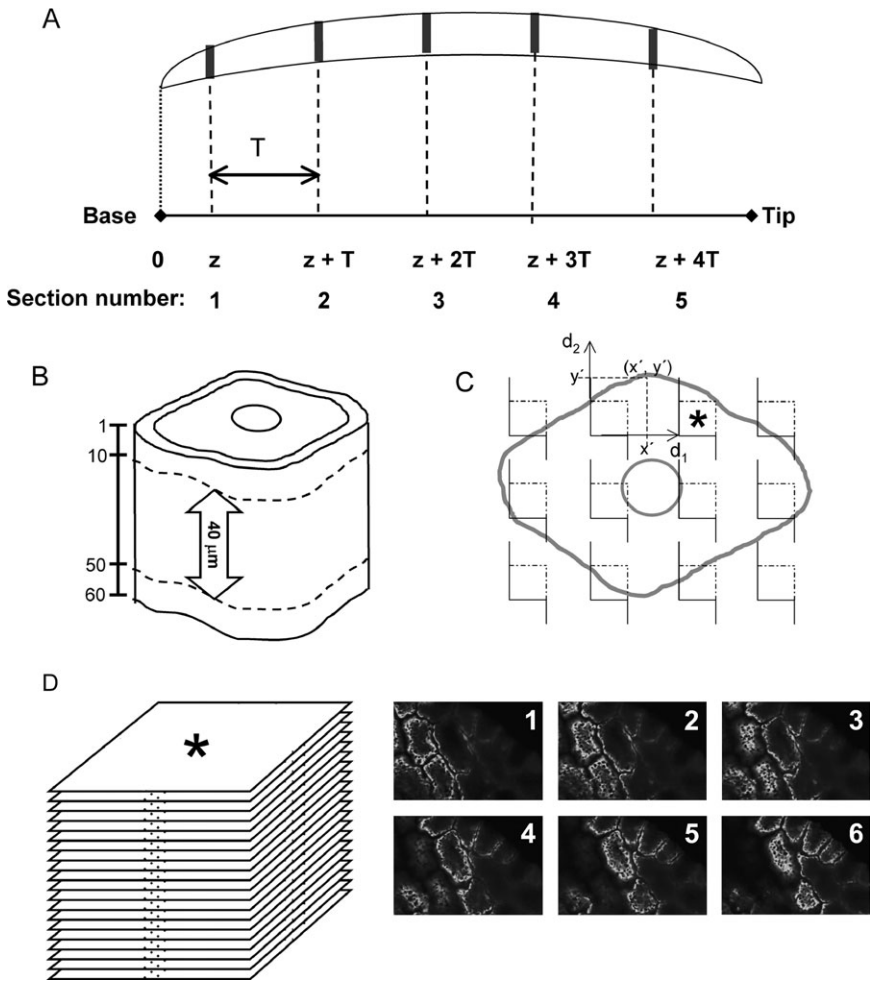

Fig. 1. Sampling design of mesophyll measurement in a Norway spruce needle. (A) Systematic uniform random sampling of the cross-sections along the needle axis. First, the interval, T, between two neighbouring cross-sections was chosen. T=2 mm here. A random number, z, determining the position of the first cross-section, was then selected within interval T. This number was selected at random from {0.5, 1, 1.5, 2} and the first section was then cut at z mm from the needle base. (B) A series of 40 optical sections 1 μm apart was acquired from the 60 μm thick cross-section using a confocal microscope. (C) Systematic sampling of unbiased sampling frames, applied to confocal series used in disector and fakir methods. The system of frames was placed on the needle section so that the uppermost point of the section lay in the position (x', y'), where x', y' were uniform random points from $(0; d_1)$ or $(0; d_2)$, respectively, d_1 and d_2 being the distances between neighbouring frames. (D) Series of optical sections acquired from the sampling frame marked by an asterisk in case (C) and an example of six of those optical sections following each other.

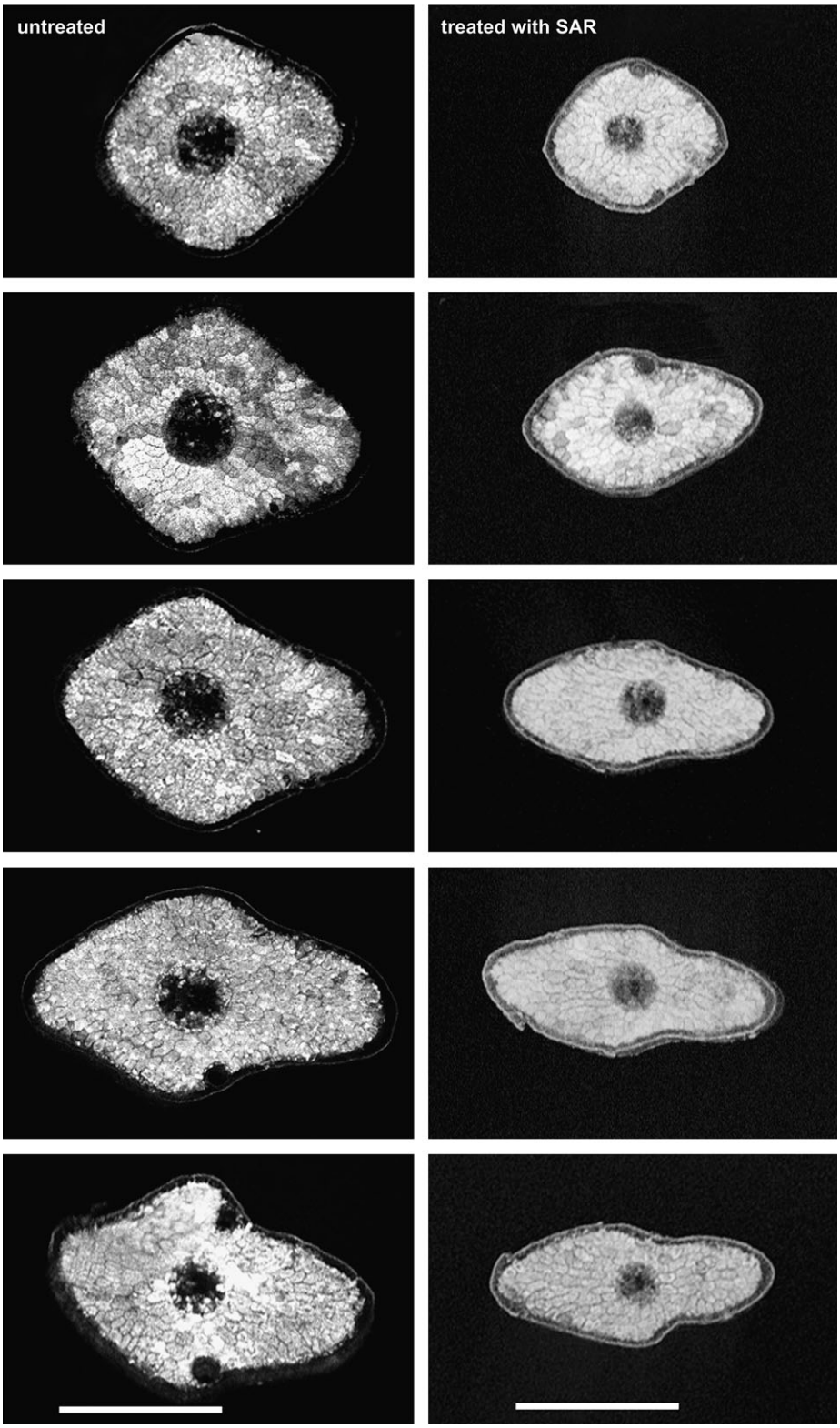

Fig. 2. Cross-sections of two Norway spruce needles acquired using a confocal microscope at systematic positions along the needle axis. The uppermost sections are located at the apex, the lowest at the needle base. Cross-sections of the needle collected before SAR treatment (left column) and a needle collected after the 1 year SAR treatment (the right column) are shown. Scale=500 μm.

Stereological methods for measuring needle structural parameters

The images of whole systematic sections of the needle (Fig. 2) were used to measure needle volume according to the Cavalieri principle (Gundersen and Jensen, 1987; Kubínová, 1993), where the total area of needle sections was multiplied by the distance between neighbouring sections. The images were also used to measure the volume density of mesophyll according to the point-counting method (Weibel, 1979; Kubínová, 1993). At the same time, the point-counting method was applied to the estimation of cross-sectional areas of the needle, mesophyll, central cylinder, and epidermis, together with hypodermis at different positions along the needle axis.

For all remaining measurements, the stacks of serial confocal sections, sampled as shown in Fig. 1C, were used to provide a higher lateral and axial resolution needed to evaluate the more subtle mesophyll structures.

First, the optical disector method was applied, yielding the number of mesophyll cells in a needle, mean mesophyll cell volume, and the ratio of intercellular spaces per mesophyll cell volume. The FAKIR and SANDAU programs written in TurboPascal 6 for IBM PC under the MS DOS operating system (available as a freeware via Internet at website http://www.biomed.cas.cz/fgu/fakir/3dtools.htm) or the DISECTOR module running in the *Ellipse* (ViDiTo, Slovakia) environment were used.

The optical disector (Gundersen, 1986) is based on focusing through the 3D probe within a thick section. Think of it as a box-shaped piece cut from jelly filled with raisins; some of the raisins are cut by the cover, sides, and bottom of the box. The whole raisins that are lying within the box are certainly counted but what about those that were cut in two by the box sides? The proper method is to count only those that are intersected by the bottom, right, and back of the box, and exclude those intersected by the remaining three sides. In the present case, where there is a thick needle section with mesophyll cells instead of jelly with raisins, a counting frame can be placed on the needle slice and, by focusing through the tissue, the 'virtual' box of tissue is obtained. The contents of the box of tissue can then be viewed by browsing through a stack of optical sections captured by a confocal microscope. During focusing up from the bottom, only those mesophyll cells within the box that disappear during focusing (i.e. those not intersected by the upper side) and at the same time are not intersected by the left and front sides of the virtual box (i.e. their sections are not intersected by the exclusion lines of the unbiased counting frame, see Fig. 3) are counted. After applying the disector probes in all sampled stacks of confocal sections in each needle (Fig. 1C), the total number of mesophyll cells in the needle, $N(mes.cell)$, was estimated using the formula:

$$estN(mes.cell) = \frac{Q^{-}(mes.cell)}{P(needle)} \cdot \frac{p}{a' \cdot h} \cdot V(needle) \qquad (1)$$

where $Q^{-}(mes.cell)$ is the number of mesophyll cells sampled by all disector boxes in the needle, p is the number of grid test points on one sampling frame, $P(needle)$ is the total number of grid test points found on the needle in all sampling frames, a' is the actual area of one sampling frame, h denotes the height of the disector box, and $V(needle)$ is the volume of the needle. To increase the efficiency of measurement, the disector boxes were applied in both directions, i.e. the cells were counted during focusing up from the bottom and then down from the top of the disector box. The grid test points found on the needle were also counted twice, first in the bottom level of the disector box and then also at its top level (Fig. 3). The height of the disector probe, h, was chosen to be 30 mm. The probe was placed in the middle of the stack of optical sections, leaving a guarding volume above and below the disector box. The actual area of one sampling frame, a', was 18 300 μm^2, and six grid test points were placed on one frame, i.e. p=6.

The mean mesophyll cell volume in the needle was estimated using a similar measurement with the same disector probes:

$$est\ \bar{v}_N(mes.cell) = \frac{P(mes.cell)}{Q^{-}(mes.cell)} \cdot \frac{a' \cdot h}{p} \qquad (2)$$

where $P(mes.cell)$ is the number of points of the p-point grid (p=6) found on the particle profiles in all sampling frames evaluated for the needle under study.

The ratio of intercellular spaces per mesophyll cell volume was measured using a point-counting method utilizing the same point grid and test frames selected for the disector measurements applied to one level of each disector box. The test points falling within the intercellular spaces were counted and divided by the number of test points found in the mesophyll cells.

The internal surface area of the needle, $S(int)$, was estimated using the fakir method (Kubínová and Janáček, 1998). The fakir method uses systematic probes consisting of parallel test lines (resembling nails of a fakir bed piercing the surface). When estimating the internal surface area of the needle, $S(int)$, the intersections between the mesophyll cell walls exposed to intercellular spaces and the fakir probes were counted (Fig. 4). It can be imagined that the cells were pierced through by the nails of the fakir bed and the number of times the nails went into or out of the exposed cell walls was counted. To increase the efficiency of the measurement, a cubic spatial grid consisting of three mutually perpendicular fakir probes was used, halfway shifted with respect to each other (Fig. 5; Kubínová and Janáček, 1998). The internal surface area of the needle, $S(int)$, was then estimated using the formula:

$$estS(int) = \frac{2}{3} \cdot u^2 \cdot (I_1 + I_2 + I_3) \qquad (3)$$

where u is the distance between neighbouring parallel lines of the grid and I_j (j=1, 2, 3) is the number of intersections between the jth fakir probe and the surface of the exposed mesophyll cell walls in all series from the given needle, sampled as shown in Fig. 1C. The measurement was easily performed using the FAKIR program written in TurboPascal 6 for IBM PC under the MS DOS operating system (available as freeware via the Internet at website http://www.biomed.cas.cz/fgu/fakir/3dtools.htm) or the FAKIR module running in the *Ellipse* (ViDiTo, Slovakia) environment. This software generates an isotropic set of virtual fakir probes and so it is not necessary to randomize the direction of the stack of sections.

The above parameters of needles before and after 1 year of acid rain treatment were compared. Further, selected parameters were compared with respect to the positions of transverse sections along the needle longitudinal axis to see if they are constant or variable along the needle.

Statistical analysis was performed using a paired t-test and one-way ANOVA, α level=0.05, and a Tukey–Kramer multiple comparison test if the data were normally distributed; otherwise the Kruskal–Wallis Z-test was applied.

Results

According to the tests with needle transverse sections of different thickness, 60 μm thick sections were found to be optimal for capturing a series of 40 optical sections 1 μm apart with sufficiently high resolution to conduct

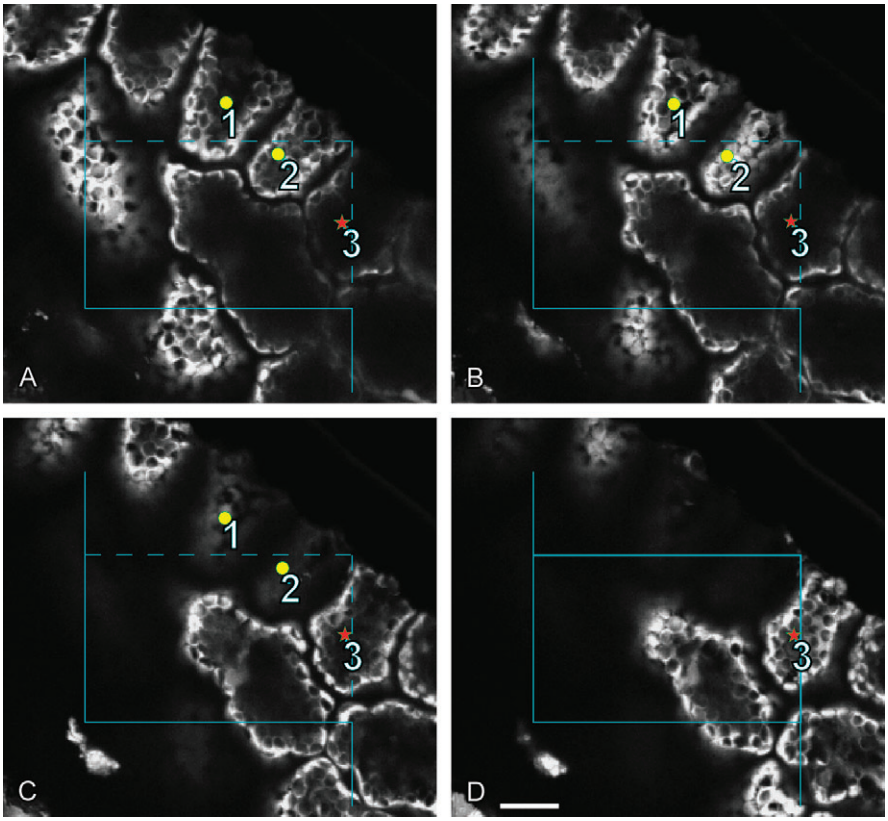

Fig. 3. Counting mesophyll cells of the Norway spruce needle using the optical disector method (A–D); Four serial sections of mesophyll cells, 3 μm apart, are shown. In (A), three cell profiles are sampled using the unbiased sampling frame (the cell profiles must not be intersected by the filled exclusion line). During focusing through, cells nos 1 and 2 disappear, i.e. they do not intersect the look-up, exclusion plane in (D), and they are not intersected by exclusion lines either. Thus, these two cells (marked by yellow points) are sampled by the disector. On the other hand, cell no. 3 (marked by a red asterisk) is still seen in the exclusion plane (D) and so it is not counted. Scale bar=50 μm.

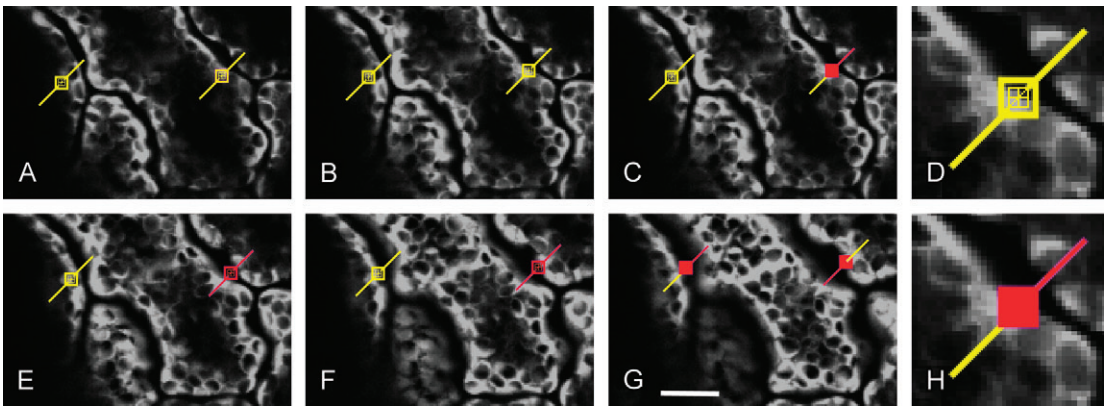

Fig. 4. Fakir method applied to estimate the area of exposed surface of mesophyll cells in a Norway spruce needle using the FAKIR program. The procedure is shown in four subsequent optical sections. The first optical section is shown in (A), the second one in (B) and (C), the third one in (E), and the last one in (F) and (G). The test lines of the fakir probe piercing the mesophyll cells are yellow at the beginning of the measurement (A). The centres of yellow squares denote the intersection points between the test lines and the current section. As soon as such a point comes into contact with the cell wall during focusing through (B, D), it is marked by a mouse and the square is filled with red (C, H); the part of the test line above this point also becomes red (C, H). Altogether three intersection points were marked here. The scale bar in G corresponds to 50 μm for (A, B, C, E, F, and G). In (D) and (H), details from (B) and (C) are shown, magnified ×3.

stereological measurements (Fig. 1B). Thinner sections would not enable the minimalization of the effect of possible distortions of section-cutting surfaces. Sections thicker than 80 μm, however, caused problems with image acquisition when using the confocal microscope due to the limited working distance of the water immersion objective used.

Results for stereological parameters of the Norway spruce needles and their mesophyll anatomical structure obtained using this study's novel stereological methods are shown in Table 1. The comparison of selected mesophyll parameters was conducted to evaluate the effect of simulated acid rain on current Norway spruce needles. Although the needle length did not differ between treated and untreated needles, needle volume significantly decreased after SAR application due to the decrease of cross-sectional area of treated needles (Fig. 2). The volume density of mesophyll did not change significantly after the treatment, while the volume of intercellular spaces per mesophyll cell volume increased, which corresponded well to the decrease in the number of mesophyll cells per unit volume of the needle. Also the total number of mesophyll cells decreased in treated needles. No significant change in mean mesophyll cell volume was observed. The internal surface area of a needle decreased after the SAR application, but the internal needle surface area per unit needle volume increased (Table 1).

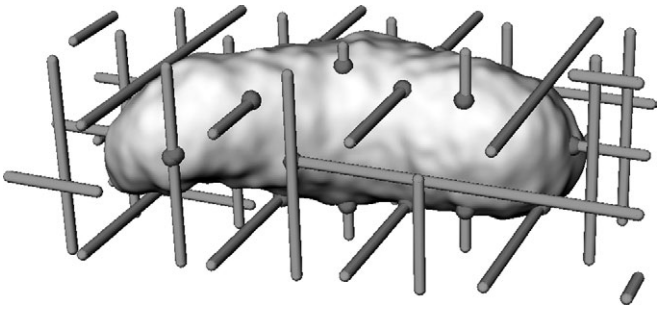

Fig. 5. Fakir probe intersecting an isolated mesophyll cell. The balls denote the intersection points between the test lines and the cell surface.

Further, selected needle anatomical parameters obtained using classical stereological methods in cross-sections cut at different positions along the needle longitudinal axis were compared (Fig. 6). Needle and mesophyll cross-sectional area were significantly higher in the middle positions of the needle than at the base and apex, while the area of epidermis and hypodermis or central cylinder did not display significant differences with respect to the cross-section position. The number of mesophyll cells per unit needle volume and mean mesophyll cell volume did not differ between the cross-section positions (Fig. 7). The effect of the cross-section position on the ratio of intercellular spaces per mesophyll cell volume and

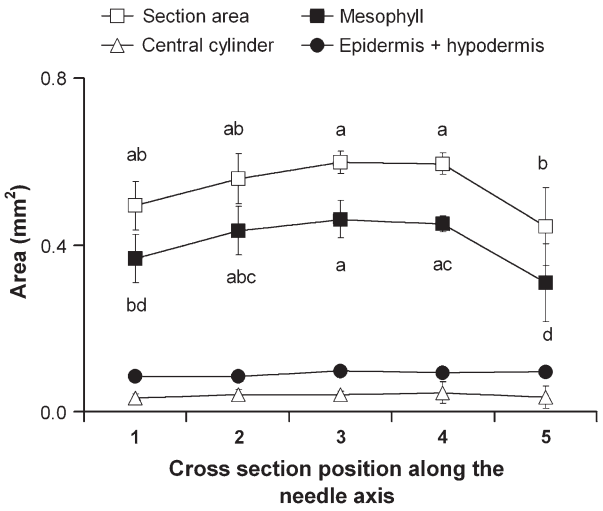

Fig. 6. Cross-sectional areas of the needle, mesophyll, central cylinder, and epidermis together with hypodermis at different positions along the needle axis of a current year Norway spruce needle treated for 1 year with simulated acid rain. Numbers on the *x*-axis refer to the five positions of the cross-sections along the needle axis beginning from the base of the needle. Bars show the standard deviation; different letters indicate significant differences at α=0.05, one-way ANOVA.

Table 1. *Mean values of 3D structural parameters of mesophyll for current year Norway spruce needles*

Values for untreated needles and needles treated with 1 year of simulated acid rain (SAR). Paired *t*-test, n=5 needles per treatment.

	Untreated needles (1999)		Treated needles (2000)		SAR effect[a]
	Mean	SD	Mean	SD	
Needle length (mm)	10.80	0.837	10.10	0.224	NS
Needle volume (mm^3)	6.19	0.735	3.41	0.417	**
Volume density of mesophyll	0.79	0.132	0.80	0.047	NS
Volume density of intercellular spaces in mesophyll	0.23	0.101	0.45	0.107	*
No. of mesophyll cells per unit volume of the needle (mm^{-3})	6508	914	4636	686	*
Mean mesophyll cell volume (μm^3)	109 060	31 028	148 540	29 678	NS
No. of mesophyll cells in a needle	40 206	7109	15 748	2700	**
Internal surface area of a needle (mm^2)	57.42	8.983	39.15	8.739	**
Internal needle surface area per unit needle volume (mm^{-1})	9.46	2.271	11.42	1.288	*

[a] *Significant at $P \leq 0.05$; **Significant at $P \leq 0.01$; ns, not significant.

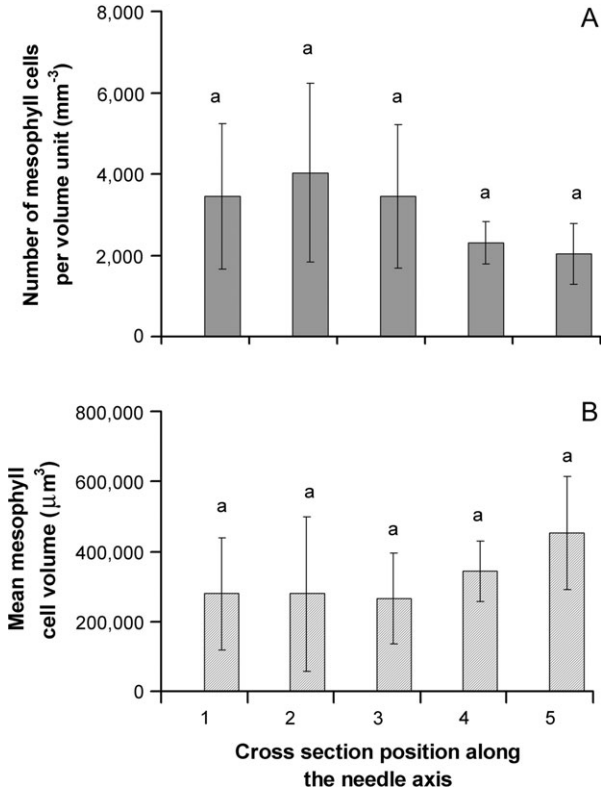

Fig. 7. Number of mesophyll cells per unit needle volume (A) and mean mesophyll cell volume (B) measured in different positions along the needle axis of a current year Norway spruce needle treated with simulated acid rain for 1 year. Numbers on the *x*-axis refer to the five positions of the cross-sections along the needle axis beginning from the base of the needle. Bars show the standard deviation; identical letters show no significant differences at α=0.05, one-way ANOVA.

internal surface density was also tested, but the data showed very high variability in the sample studied and thus the results were not found to be reliable.

Discussion

The present study proved the feasibility of methods of confocal stereology for efficient measurement of stereological parameters characterizing the anatomical structure of Norway spruce needles. It was shown that not only can the recently developed methods based on evaluation of 3D image data be successfully applied to needle structure analysis but also classical stereological methods can be easily applied to images captured using confocal microscopy. The present methods can be directly used for quantitative anatomical studies of other coniferous needles and other types of narrow leaves and, after slight modifications, also for the analysis of leaves of different shapes, for example, broad bifacial leaves where different sampling of leaf segments and transverse thick sections would be applied, as indicated in Kubínová (1993). The methods can also be easily modified to evaluate other plant organs, such as roots and stems.

Thin optical sections can be acquired in conventional light microscopy when using a lens with a high numerical aperture; however, observation of deeper layers in fresh thick sections is not possible due to the blur from out-of-focus specimen layers. If an objective with a low numerical aperture, i.e. a higher depth of focus, is used, several cell layers are displayed on the final observed projection, which also makes measurements difficult. Confocal microscopy enables the acquisition of thin optical sections within a thick physical section; thus, details of tissue arrangement are revealed. Plant material, containing autofluorescent components, is very suitable for fluorescence microscopy in plant anatomy studies even without any special staining. In leaves, the autofluorescence of chloroplasts containing photosynthetic pigments and of phenolic compounds localized either in cell walls or in vacuoles abundant in certain leaves, such as needles of Norway spruce (Soukupová *et al*., 2000), can be exploited.

Most studies on foliar internal structure use sections of fixed and embedded plant material (Turrell, 1936; Eguchi *et al*., 2004; Pandey and Kushwaha, 2005); however, during fixation or embedding, tissue deformation and other artefacts may occur (Uwins *et al*., 1993). Therefore, another advantage of using free-hand sections of fresh needles is the elimination of such deformation problems. Distortions of cutting surfaces of transversely cut needle sections, however, are likely to occur because conifer needles exhibit the arrangement of mesophyll cells in transversally oriented interconnected layers (Esau, 1953). The location of the disector and fakir probes within the stack of optical sections could play a role in overcoming the observed variability, and will be tested further. Using fresh material can limit the application of the method in experimental research because only a few needles can be analysed simultaneously—processing of one needle including sectioning and image acquisition took ~4 h in the present study. This problem could be solved if a suitable form of storage of sampled material is found. The easiest way would be freezing, provided the thawing does not cause structural deformations, which is now being studied, as is the effect of possible deformations due to the cutting of unembedded material.

In many physiological studies conducted on conifers, only cross-sections from the middle part of the needle are used to measure needle and mesophyll geometrical parameters (e.g. Apple *et al*., 2002), without checking that this specific position is representative for the entire needle. The differences in the cross-sectional area along the needle axis were shown in a recent study (Lhotáková *et al*., 2006), when parameters of cross-sections sampled in the middle part of the needle differed from those sampled at the tip and base. In the present study, however,

special mesophyll structural parameters, such as the number of mesophyll cells per needle volume and mean mesophyll cell volume, did not change with the cross-section position. Zwieniecki *et al*. (2006) also observed constant needle parameters along 80% of the needle axis on needles of three pine species. Thus, the evaluation of sections taken only in the middle part of the needle can be sufficient to obtain reliable results, which is useful especially in more extensive physiological studies. However, the variability along the needle axis should be verified for each specific anatomical parameter and variant.

A model-based approach, when assumptions about mesophyll cell shapes are made, is still commonly used to determine mesophyll structural parameters (for recent applications, see Slaton and Smith, 2002; Rhizoupoulou and Psaras, 2003; Barbour and Farquhar, 2003; Pandey and Kushwaha, 2005). Some of the pitfalls of approximating cells by geometrical solids were pointed out by Kubínová (1993, 1994) and Slaton and Smith (2002), stressing inaccuracy especially in surface area measurements. Norway spruce mesophyll cells have an irregular lobed shape, and thus modelling them with cylinders or other geometrical bodies is not appropriate, and yields biased results. Therefore, only design-based methods appear to be suitable for unbiased estimation of mesophyll geometrical parameters. Many of the difficulties connected with the implementation of classical design-based stereological methods for estimating needle mesophyll parameters are overcome by the presented approach using confocal microscopy, also resulting in much faster measurements. In the case of internal needle surface area measurement, the analysis was more than three times faster when compared with the implementation of the method of vertical sections (Kubínová, 1991, 1993). The time efficiency of the new approach is further increased by the possibility of using the same stacks of confocal sections for measurements of different parameters, i.e. mean mesophyll cell volume, mesophyll cell number in a needle, and internal surface area of needles, as well as the ratio of intercellular spaces per mesophyll cell volume.

Only a few studies using stereological methods based on 3D probes, such as a disector, to obtain a detailed description of internal leaf structure have been published. The optical disector method was successfully applied to paraffin sections of grass leaves when a 3D disector probe was placed by optical sectioning within one 20 μm thick physical section (Albrechtová and Kubínová, 1991; Kubínová, 1991). To our knowledge, the fakir method has yet to be used in any plant anatomy study.

Conifer needle anatomy has been predominantly studied for Norway spruce since the 1980s, mainly due to the widespread forest decline caused by atmospheric pollution and acid rain (Albrechtová *et al*., 2001). However, most studies describe the anatomical alterations only qualitatively, for example, by the presence of collapsed cells (Kukkola *et al*., 2005) or loss of chloroplasts (Moss *et al*., 1998). In the present study, the purpose was to test if the confocal stereology analysis is capable of capturing subtle changes in mesophyll arrangement. To reduce variability of plant material, it was decided to analyse needles only from the same branch. To induce the subtle changes, a treatment with simulated acid rain was used as a stress factor, which is known to cause damage in the mesophyll with already described symptoms, such as a decrease in needle length and volume or an increase of the volume of the intercellular spaces (Masuch *et al*., 1992). The significant decrease of needle volume was detected as the effect of SAR treatment, which was caused by a reduced area of the needle cross-sections, while needle length remained unchanged. Needle thinning, expressed as lower cross-sectional area, was already documented in Norway spruce needles collected from a heavily polluted site in comparison with needles collected from a healthy site (Masuch *et al*., 1992). Similarly, as reported by Masuch *et al*. (1992), the volume of intercellular spaces per mesophyll cell volume increased after acid rain application. By contrast, Kukkola *et al*. (2005), who assessed the proportion of intercellular spaces using the point-counting method on semi-thin sections of Scots pine needles treated with simulated acid rain, found no effect of SAR on the extent of intercellular spaces. Moss *et al*. (1998), however, detected large cavities in red spruce mesophyll caused by the acid mist event, which corresponds to the present finding of increased volume of intercellular spaces after the SAR treatment.

Differences in mesophyll architecture, such as leaf porosity expressed as volume percentage of intercellular spaces in mesophyll, are important for evaluating the impact of internal leaf surface area or chloroplast area available for CO_2 absorption during photosynthesis (Slaton and Smith, 2002). The relationships between the structural arrangement of mesophyll and leaf reflectance could bring new tools for monitoring photosynthetic performance using remote sensing methods. Slaton *et al*. (2001) found a strong correlation between the ratio of mesophyll cell surface area exposed to intercellular air spaces expressed per unit leaf area and reflectance in near infrared (800 nm) for 48 alpine herbaceous species.

Models of major features of leaf photosynthesis based on mathematical description of leaf gas exchange, electron transport, and biochemistry that were developed in the last three decades stimulated development in understanding the physiology of photosynthesis and methodology of photosynthetic measurements (Farquhar *et al*., 2001). The modelling of canopy photosynthesis, however, also requires more detailed knowledge on relationships between photon interactions and leaf structure, leaf orientation, and photosynthetic potential, which can be obtained from a quantitative description of a 3D structure of plant

tissue by using simulation (Ustin *et al*., 2001). This recent development in interpretation of structure–function relationships in a leaf indicates that quantitative ultrastructural studies, similar to those presented herein, are of fundamental importance in understanding photosynthesis at the leaf and canopy level. Thus, detailed and unbiased estimators of mesophyll parameters are becoming crucial for modelling physiological processes that underlie photosynthesis, such as gas transport (Aalto and Juurola, 2002; Juurola *et al*., 2005) or radiative transfer (Ustin *et al*., 2001). It is believed that the present stereological analysis is a promising new tool for plant physiological and modelling research.

Acknowledgements

Supported by the Ministry of Youth and Education of the Czech Republic (grant LC06063), and the Academy of Sciences of the Czech Republic (grants A5011810, A600110507, and AV0Z50110509). We thank Janice Forry for proofreading the manuscript and help with the English.

References

Aalto T, Juurola E. 2002. A three-dimensional model of CO_2 transport in airspaces and mesophyll cells of a silver birch leaf. *Plant, Cell and Environment* **25,** 1399–1409.

Albrechtová J, Kubínová L. 1991. Quantitative analysis of the structure of etiolated barley leaf using stereological methods. *Journal of Experimental Botany* **42,** 1311–1314.

Albrechtová J, Rock BN, Soukupová J, Entcheva P, Šolcová B, Polák T. 2001. Biochemical, histochemical, structural and reflectance markers of damage in Norway spruce from the Krušné hory used for interpretation of remote sensing data. *Journal of Forest Science* **47,** 26–33.

Apple M, Tiekotter K, Snow M, Young J, Soeldner A, Phillips D, Tingey D, Bond BJ. 2002. Needle anatomy changes with increasing tree age in Douglas-fir. *Tree Physiology* **22,** 129–136.

Barbour MM, Farquhar GD. 2003. Do pathways of water movement and leaf anatomical dimensions allow development of gradients in $H_2^{18}O$ between veins and the sites of evaporation within leaves? *Plant, Cell and Environment* **27,** 107–121.

Chabot BF, Chabot JF. 1977. Effects of light and temperature on leaf anatomy and photosynthesis in *Fragaria vesca*. *Oecologia (Berlin)* **26,** 363–377.

Chonan N. 1965. Studies on the photosynthetic tissues in the leaves of cereal crops. I. The mesophyll structure of wheat leaves inserted at different levels of the shoot. *Proceedings of the Crop Science Society of Japan* **33,** 388–393.

Eguchi N, Fukatsu E, Funada R, Tobita H, Kitao M, Maruyama Y, Koike T. 2004. Changes in morphology, anatomy, and photosynthetic capacity of needles of Japanese larch (*Larix kaempferi*) seedlings grown in high CO_2 concentrations. *Photosynthetica* **42,** 173–178.

Esau K. 1953. *Plant anatomy*. New York: John Wiley & Sons.

Farquhar GD, von Caemmerer S, Berry JA. 2001. Models of photosynthesis. *Plant Physiology* **125,** 42–45.

Gundersen HJG. 1986. Stereology of arbitrary particles. A review of unbiased number and size estimators and the presentation of some new ones, in the memory of William R. Thompson. *Journal of Microscopy* **143,** 3–45.

Gundersen HJG, Jensen EB. 1987. The efficiency of systematic sampling in stereology and its prediction. *Journal of Microscopy* **147,** 229–263.

Howard CV, Reed MG. 1998. *Unbiased stereology: three-dimensional measurement in microscopy*. *Microscopy handbooks*, Vol. 41. New York: Springer-Verlag.

Howard CV, Reid S, Baddeley A, Boyde A. 1985. Unbiased estimation of particle density in the tandem scanning reflected light microscope. *Journal of Microscopy* **138,** 203–212.

Howard CV, Sandau K. 1992. Measuring the surface area of a cell by the method of the spatial grid with a CSLM—a demonstration. *Journal of Microscopy* **165,** 183–188.

Juurola E, Aalto T, Thum T, Vesala T, Hari P. 2005. Temperature dependence of leaf-level CO_2 fixation: revising biochemical coefficients through analysis of leaf three-dimensional structure. *New Phytologist* **166,** 205–215.

Kubínová L. 1991. Stomata and mesophyll characteristics of barley leaf as affected by light–stereological analysis. *Journal of Experimental Botany* **42,** 995–1001.

Kubínová L. 1993. Recent stereological methods for the measurement of leaf anatomical characteristics: estimation of volume density, volume and surface area. *Journal of Experimental Botany* **44,** 165–173.

Kubínová L. 1994. Recent stereological methods for measuring leaf anatomical characteristics: estimation of the number and sizes of stomata and mesophyll cells. *Journal of Experimental Botany* **45,** 119–127.

Kubínová L, Janáček J. 1998. Estimating surface area by the isotropic fakir method from thick slices cut in an arbitrary direction. *Journal of Microscopy* **191,** 201–211.

Kubínová L, Janáček J, Guilak F, Opatrný Z. 1999. Comparison of several digital and stereological methods for estimating surface area and volume of cells studied by confocal microscopy. *Cytometry* **36,** 85–95.

Kubínová L, Janáček J, Krekule I. 2002. Stereological methods for estimating geometrical parameters of microscopical structure studied by three-dimensional microscopical techniques. In: Diaspro A, ed. *Confocal and two-photon microscopy*. New York: Wiley-Liss, 299–332.

Kukkola E, Rautio P, Huttunen S. 2005. Long-term symptoms due to metal and acid precipitation treatments in Scots pine (*Pinus sylvestris*) needles in the subarctic. *Arctic, Antarctic, and Alpine Research* **37,** 68–74.

Lhotáková Z, Albrechtová J, Malenovský Z, Rock BN, Polák T, Cudlín P. 2006. Does the azimuth orientation of Norway spruce (*Picea abies* L. Karst.) branches within sunlit crown influence the heterogeneity of biochemical, structural and spectral characteristics of needles? *Environmental and Experimental Botany* (in press).

Lieckfeldt E. 1989. Importance of leaf anatomy for characterization of primary leaf photosynthetic efficiency in different genotypes of wheat (*Triticum*). *Photosynthetica* **23,** 63–70.

Maksymowych R. 1959. Quantitative analysis of leaf development in *Xanthium pensylvanicum*. *American Journal of Botany* **46,** 635–644.

Masuch G, Franz JT, Kicinski HG, Kettrup A. 1992. Histological and biochemical differences of slightly and severely injured spruce needles of two stands in Northrhine Westphalia. *Environmental and Experimental Botany* **32,** 163–182.

Moss DM, Rock BN, Bogle AL, Bilkova J. 1998. Anatomical evidence of the development of damage symptoms across a growing season in needles of red spruce from central New Hampshire. *Environmental and Experimental Botany* **39,** 247–262.

Pandey S, Kushwaha R. 2005. Leaf anatomy and photosynthetic acclimation in *Valeriana jatamansi* L. grown under high and low irradiance. *Photosynthetica* **43,** 85–90.

Parkhurst DF. 1982. Stereological methods for measuring internal leaf structure variables. *American Journal of Botany* **69,** 31–39.

Pawley JB. (ed.) 1995. *Handbook of biological confocal microscopy*, 2nd edn. New York: Plenum Press.

Pazourek J. 1977. The volumes of anatomical components in leaves of *Typha angustifolia* L. and *Typha latifolia* L. *Biologia Plantarum* **19,** 129–135.

Pazourek J. 1988. The evolution of quantitative plant anatomy. *Acta Universitatis Carolinae – Biologica* **31,** 15–25.

Rhizoupoulou S, Psaras GP. 2003. Development and structure of drought-tolerant leaves of the Mediterranean shrub *Capparis spinosa* L. *Annals of Botany* **92,** 377–383.

Sasahara T. 1982. Genetic variations in cell and tissue forms in relation to plant growth. II. Total cell surface area in the palisade parenchyma and total cell surface area:total nitrogen content ratio in relation to photosynthetic activity in *Brassica*. *Japanese Journal of Breeding* **21,** 61–68.

Slaton MR, Hunt ER, Smith WK. 2001. Estimating near-infrared leaf reflectance from leaf structural characteristics. *American Journal of Botany* **88,** 278–284.

Slaton MR, Smith WK. 2002. Mesophyll architecture and cell exposure to intercellular air space in alpine, desert, and forest species. *International Journal of Plant Sciences* **163,** 937–948.

Soukupová J, Cvikrová M, Albrechtová J, Rock BN, Eder J. 2000. Histochemical and biochemical approaches to the study of phenolic compounds of Norway spruce (*Picea abies*). *New Phytologist* **146,** 403–414.

Sterio DC. 1984. The unbiased estimation of number and sizes of arbitrary particles using the disector. *Journal of Microscopy* **134,** 127–136.

Turrell FM. 1936. The area of the internal exposed surface of dicotyledon leaves. *American Journal of Botany* **23,** 255–264.

Ustin SL, Jacquemoud S, Govaerts Y. 2001. Simulation of photon transport in a three-dimensional leaf: implications for photosynthesis. *Plant, Cell and Environment* **24,** 1095–1103.

Uwins PJR, Murray M, Gould RJ. 1993. Effects of four different processing techniques on the microstructure of potatoes: comparison with fresh samples in the ESEM. *Microscopy Research and Technique* **25,** 412–418.

Vávra V. 1992. *Kvalita vody Labe v pramenné oblasti: stav, příčiny a důsledky na biocenózu*. Vrchlabí: Administration of the Krkonoše National Park [In Czech] (Water quality of the river Elbe in the source area: state, causes and conseqeunces for biocoenosis). Scientific report.

Weibel ER. 1979. *Stereological methods*. Vol. 1. *Practical methods for biological morphometry*. London: Academic Press.

Wilson D, Cooper JP. 1967. Assimilation of *Lolium* in relation to leaf mesophyll. *Nature* **214,** 989–992.

Zwieniecki MA, Stone HA, Leigh A, Boyce KC, Holbrook M. 2006. Hydraulic design of pine needles: one-dimensional optimization for single-vein leaves. *Plant, Cell and Environment* **29,** 803–809.